Environ Earth Sci (2011) 64:851–859
DOI 10.1007/s12665-011-0909-z

ORIGINAL ARTICLE

Identifying spatial patterns of synchronization between NDVI and climatic determinants using joint recurrence plots

Shuangcheng Li · Zhiqiang Zhao · Yang Wang · Yanglin Wang

Received: 22 March 2010 / Accepted: 4 January 2011 / Published online: 8 February 2011

Abstract Ten-day series of the Normalized Difference Vegetation Index (NDVI) derived from multi-temporal satellite imagery (1998–2008) was employed as a surrogate for the surface vegetation cover to investigate synchronization of the climatic determinants and its spatial patterns in China. The results, both of the spatiotemporal patterns of joint probability of recurrence (JPR) index and lag time of maximal JPR, clearly suggest that the synchronous relationships of NDVI–climate are site specific and spatially heterogeneous. Higher JPR values of NDVI–temperature are found in Northern China, indicating stronger synchronization in these areas, while higher JPR values of NDVI–precipitation are found in semi-arid and semi-humid regions, which suggest that the moisture factor has a significant influence on NDVI in these areas. Whether lagged or advanced relationship, the phase difference of NDVI–temperature is smaller in Southern China, while is bigger in Northern China. In contrast, the phase difference of NDVI–precipitation is smaller in the semi-arid and sub-humid areas, which means that precipitation has a significant and immediate influence on vegetation in these areas. Overall, the JPR values for NDVI–temperature are higher than those for NDVI–precipitation, suggest that the synchronization between NDVI and temperature is stronger than that between NDVI and precipitation in most areas of China. The results indicate that joint recurrence quantification analysis is a good candidate method for identifying the synchronization between NDVI and climatic determinants.

S. Li (✉) · Z. Zhao · Y. Wang · Y. Wang
Laboratory for Earth Surface Processes Ministry of Education, College of Urban and Environmental Sciences, Peking University, Beijing 100871, China
e-mail: scli@urban.pku.edu.cn

Keywords Joint recurrence plots · NDVI · Climatic determinants · Synchronization · Joint probability of recurrence

Introduction

Vegetation monitoring is essential for dealing with many environmental issues such as biodiversity conservation, global climate change and ecosystem management. Because the Normalized Difference Vegetation Index (NDVI), a parameter derived from red and near-infrared reflectance, is a good indicator of terrestrial vegetation distribution and productivity (Goward et al. 1985; Tucker et al. 1985), it has been widely employed to develop correlated and dependent relationships with the climatic factors (Malo and Nicholson 1990; Di et al. 1994; Yang et al. 1998; Fang et al. 2001; Ichii et al. 2002; Kaufmann et al. 2003; Ji and Peters 2004; Xiao and Moody 2004; Anyamba and Tucker 2005; Funk and Brown 2006; Propastin et al. 2008; Tourre et al. 2008; Udelhoven et al. 2009; Torres and Gamero 2000). Traditionally, general correlation and linear regression analysis are the major techniques to explore relationships between NDVI and climatic factors. However, when the NDVI–climate relationships reveal complex features such as nonlinearity and non-stationarity, those conventional methods might fail to detect causality because their underlying assumption of linearity is violated, resulting in poor insights regarding the evolution trends of vegetation cover and underlying physical processes. Moreover, while the NDVI–climate relationships have been extensively studied, particularly in the coarse-scales, little efforts have been made to explicitly investigate their coupling and synchronization. Understanding the phase coherency hidden in NDVI and climatic factors is helpful for our ability to predict the dynamics of NDVI variation.

In recent years, some measures of nonlinear dynamics have been widely used to indicate the characteristics of nonlinear dynamic systems, such as the correlation dimension, Lyapunov exponents, Kolmogorov entropy, approximate entropy, sample entropy, and permutation entropy (Torres and Gamero 2000). Most of these approaches require a longer data series to obtain a reasonable result. In the real natural world, however, it is difficult, due to the limitation of experiment or observation conditions, to obtain a long series of ecological variable. Therefore, finding robust algorithms and measures to deal with short series and non-stationary data is still a challenging issue. In this sense, the recurrence plots (RPs), which was first introduced by Eckmann et al. (1987), are an appropriate approach. There are many reasons for choosing the RPs approach in this study, but the most important is its rapid extension to bivariate and multivariate analysis for complex systems, resulting in wide applications in various fields. For example, joint recurrence plots (JRP) and its quantitative metrics are considered a powerful tool set to deal with interrelationships among different natural systems (Romano et al. 2004). In this study, JRP measurements were introduced to quantitatively represent the coupling and synchronous relationships between NDVI and climatic determinants such as precipitation and temperature, and to examine regional differences of their synchronous relationship in China.

This paper is organized as follows. The methodology, especially the theoretical background and algorithm of RPs and JRP technique, including definition of the metrics of JRP are explained in "Methods". In "Data and preprocessing", the data and preprocessing are briefly described. In "Results", the results of investigation of spatial patterns of synchronization between NDVI and climatic determinants are presented. The last section is "Discussion and conclusion".

Methods

Recurrence plots and joint recurrence plots

The use of RPs was first proposed by Eckmann et al. (1987) to visually inspect the time dependent behavior of the dynamic system. The RPs are defined by

$$R_{i,j}(\varepsilon) = \Theta(\varepsilon - ||x_i - x_j||), \quad i,j = 1,\ldots,N \tag{1}$$

where N is the length of the measured series x_i, ε is a threshold value,$\|\cdot\|$ is a norm, and Θ $(\cdot)$ the Heaviside function (i.e., $\Theta(x) = 0$, if $x < 0$, and $\Theta(x) = 1$ otherwise). The RPs are obtained by plotting the recurrence matrix and using different colors for its binary entries, e.g., plotting a black dot at the coordinates (i, j), where $R_{i,j} = 1$, and a white dot, where $R_{i,j} = 0$. RPs yield important insights into the time evolution of phase space trajectories, because typical patterns in RPs are linked to a specific behavior of the system.

To go beyond the graphical representation and visual impression, quantitative measures for RPs were subsequently introduced, and successfully applied to many fields, such as biology (Webber and Zbilut 1994), economics (Fabretti and Ausloos 2005), ecology (Proulx et al. 2008, 2009), and earth science (Marwan et al. 2003; Li et al. 2008). In order to analyze bivariate or multivariate time series, RPs were extended to cross recurrence plot (CRP) (Zbilut et al. 1998; Marwan and Kurths 2002) and JRP (Romano et al. 2004; Marwan et al. 2007).

JRP was first introduced based on the idea of joint recurrence, which means the probability that both systems recur simultaneously to the neighborhood of a formerly visited point in their respective phase space. The joint recurrence matrix for two systems is defined as Romano et al. (2004).

$$\begin{aligned} \mathrm{JR}_{i,j}^{x,y} &= \Theta(\varepsilon^x - ||x_i - x_j||)\Theta(\varepsilon^y - ||y_i - y_j||), \\ & i,j = 1,\ldots,N, \end{aligned} \tag{2}$$

i.e.

$$\mathrm{JR}_{i,j}^{x,y} = \begin{cases} 1 & \text{if} \quad ||x_i - x_j|| < \varepsilon^x \quad \text{and} \quad ||y_i - y_j|| < \varepsilon^y \\ 0 & \text{else.} \end{cases} \tag{3}$$

The graphical representation of the matrix $\mathrm{JR}_{i,j}^{x,y}$ is called JRP. Moreover, a delayed version of the joint recurrence matrix can be easily defined by

$$\begin{aligned} \mathrm{JR}_{i,j}^{x,y} &= \Theta(\varepsilon^x - ||x_i - x_j||)\Theta(\varepsilon^y - ||y_{i+\tau} - y_{j+\tau}||), \\ & i,j = 1,\ldots,N-\tau, \end{aligned} \tag{4}$$

which can be useful for the analysis of interacting delayed systems, or even for systems with feedback (Romano et al. 2004).

JRP is an appropriate method to investigate real natural processes due to the following advantages: though both systems have different dimensions as well as physical units of each component of the system, the JRP is still well defined. In addition, the JRP is invariant under permutation of the coordinates in one or both of the considered systems, and the lines of slope 1 are still directly related to the predictability of the system.

The metrics of joint recurrence plots

Recurrence rate of JRP($RR^{x,y}$)

$\mathrm{RR}^{x,y}$ is the recurrence rate of the JRP of the systems x and y over time. It is an index that quantifies the degree of similarity between the respective recurrences of both systems. It compares the recurrences of each point of the first system with the local recurrences of the second system.

This index has the advantage that it distinguishes rather well between non-phrase synchronization (non-PS), phrase synchronization (PS), and generalized synchronization (GS). Analogously to RPs, $RR^{x,y}$ can be given by

$$RR^{x,y} = \frac{1}{N^2}\sum_{i,j=1}^{N}\Theta(\varepsilon^x - ||x_i - x_j||)\Theta(\varepsilon^y - ||y_{i+\tau} - y_{j+\tau}||) \quad (5)$$

If both systems x and y are independent of each other, then the average probability of a joint recurrence is given by $RR^{x,y} = RR^x\ RR^y = RR^2$. On the other hand, if both systems are in GS, then both systems are expected to have approximately the same recurrences, and hence $RR^{x,y} = RR^x = RR^y = RR$.

Joint probability of recurrence

To detect lag synchronization, Romano et al. proposed an index JPR based on the average JPR by choosing the maximum value of $S(\tau)$ and normalizing it,

$$S(\tau) = \frac{1/N^2\sum_{i,j}^{N} JR_{i,j}^{x,y}(\tau)}{RR}, \quad (6)$$

$$JPR = \max_{\tau}\frac{S(\tau) - RR}{1 - RR} \quad (7)$$

where RR is the same recurrence rate of two systems using a fixed number of nearest neighbors. JPR is equal to 1 if system x and system y are in GS, and is zero if two systems are completely independent. JPR does not require a large computational effort and the number of data points needed for the analysis is rather low (Romano et al. 2004).

Geographic information system

A geographic information system (GIS) is any system for obtaining, storing, analyzing, managing, and exporting geographically referenced data and information. GIS is a visual computer software platform that allows users to create interactive queries, analyze the spatial information, edit vector and raster data, and present the results of all these operations. In this study, ArcGIS 9.3 (ESRI Inc., 1999–2008) software was used to conduct the preprocessing of NDVI and climatic data, spatial analysis, to manage large amounts of spatial data, and to produce cartographically appealing maps for joint recurrence quantification measures.

Data and preprocessing

Meteorological data

Meteorological data required by the calculation of joint recurrence quantification analysis was obtained from the China Meteorological Administration (http://cdc.cma.gov.cn/). Among the 752 weather stations, 614 stations were selected because of short historical records or missing observations in some stations. The selected climatic elements include temperature and precipitation. To be consistent with the length of NDVI data series, the original daily temperature and precipitation data were aggregated into a 10-day time series. From 1 April 1998 to 31 December 2008, each temperature or precipitation series has 387 data points. The quality of climatic data was strictly controlled by verifying the weather confine, the weather singular value and the inner coherence.

Normalized difference vegetation index

One of the most widely used indices for green cover monitoring is the NDVI (Myneni et al. 1998; Maselli and Chiesi 2006). It is computed by the product of the ratio of two electromagnetic wavelengths (near infrared − red)/(near infrared + red). For this study, we used a NDVI time series of satellite observations at 1 km spatial and 10-day (decades) temporal resolution, covering the period from April 1998 to December 2008, produced by the Vlaamse Instelling voor Technologisch Onderzock (VITO) Image Processing Centre (Mol, Belgium) from the sensor VEGETATION on board the SPOT-4 satellite. A registered user can download the SPOT-4 VEGETATION 10-day synthesis (called "VGT-S10") NDVI data via the free VGT Website (http://free.vgt.vito.be/).

VGT-S10 NDVI products were synthesized from S1 (1-day resolution) NDVI products using a maximum value composite (MVC) algorithm (Jarlan et al. 2008). The influence of cloud cover was well reduced because the highest signal data within the 10-day observation was used as a pixel value for the 10-day synthesis data. The VGT-S10 products were compiled by merging segments (data strips) acquired over a 10-day period. All the segments of this period were compared again pixel by pixel to pick out the 'best' ground reflectance values. In addition, the processing of VGT-S10 products also included the application of corrections for radiometric, atmospheric and geometric effects.

NDVI values for each weather station were extracted in raster format from each VGT-S10 image using ArcGIS software. To reduce noise in a NDVI series, its values for a given station were derived and averaged within a 10 km buffer circle centered on a meteorological station.

Results

The spatial pattern of NDVI–climate joint recurrence rate

The spatial pattern of NDVI–temperature joint recurrence rate exhibits significant regional differentiations (Fig. 1a).

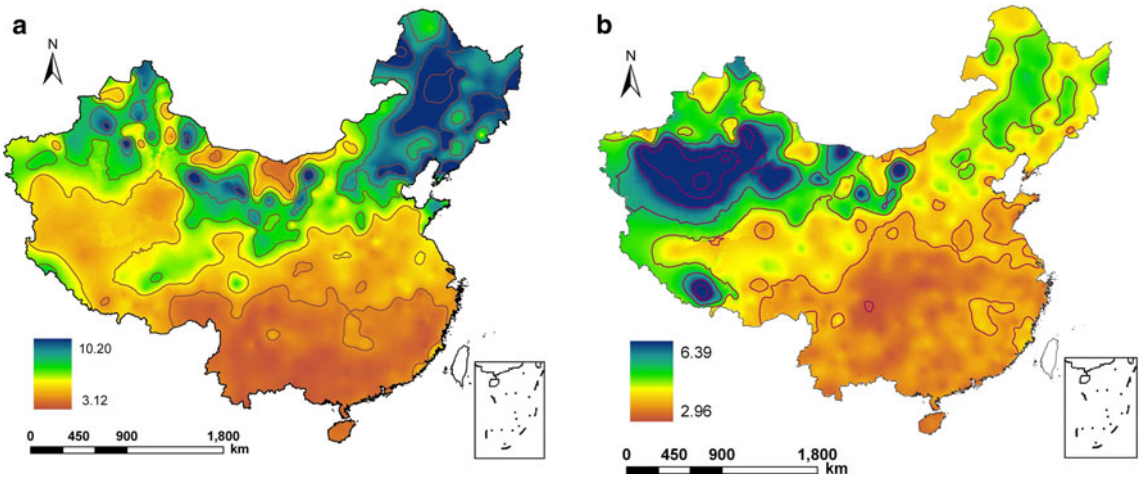

Fig. 1 The spatial pattern of NDVI–climate joint recurrence rate in China. **a** shows the spatial pattern of NDVI–temperature joint recurrence rate, and **b** shows the spatial pattern of NDVI–precipitation joint recurrence rate

The highest values of RR are observed in the northern areas of China, especially in Northeast China. In contrast, the lowest value areas are those of tropical and subtropical regions, especially in Southern China. Similar to those in Fig. 1a, the spatial pattern of NDVI–precipitation joint recurrence rate also shows geographical heterogeneity (Fig. 1b). The highest values of RR appear in the arid Northwest regions, while the lowest value areas are located in humid Southern China.

By comparing Fig. 1a and Fig. 2a it can be seen that RR values of NDVI–temperature are generally larger than those of NDVI–precipitation. This suggests that the similarity of NDVI–temperature is greater than that of NDVI–precipitation in the context of joint recurrence probability measure.

The spatial pattern of NDVI–climate synchronization

Figure 2 shows the spatial patterns of synchronized relationships between NDVI and climatic determinants, which were obtained by computing the JPR. As can be seen from Fig. 2a, tropical and subtropical wet evergreen broad-leaved forest regions show the lowest values for the JPR, while cold and dry regions in Northeastern and Northwestern China have the highest values. The spatial patterns of synchronized relationships between NDVI and precipitation exhibit marked regional differentiation (Fig. 2b). The highest JPR value areas of NDVI–precipitation appear in northeast–southwest zonal distribution, and are in agreement with the surface wet and dry features. In this zonal region, the NDVI, particularly in the central and northern sections of this region, is much more under the influence of the precipitation due to the lack of surface water and low soil moisture.

Temporal patterns of synchronous NDVI–climate relationship in selected sites

To more clearly investigate the dynamic evolution of coupling relationships between NDVI and climatic determinants in different geographical regions, four sampling sites, representing temperate deciduous broad-leaved forest, alpine meadow, subtropical evergreen broad-leaved forest, and tropical monsoon rain forest, respectively, were selected (Table 1) to compute the RR and JPR with a window size of 108 and a sliding step of 9.

Figure 3 shows the time evolution of the joint recurrence rate RR of NDVI–temperature in selected stations. Clearly, among the NDVI–temperature relationships of four stations, Station 50968 has highest RR values, suggesting the largest similarity between NDVI and temperature series in temperate deciduous broad-leaved forest region. On the contrary, NDVI and temperature in Station 58102 and Station 59278 have the lowest RR values, indicating that both series have the smallest similarity in subtropical evergreen broad-leaved forest and tropical monsoon rain forest regions. From the view of curve fluctuation and trend, throughout the period of time Station 50968 shows continuous fluctuations, while Station 56074 exhibits significant decline. In contrast, Station 58102 and Station 59278 have relatively small amplitude and smooth evolution. In Fig. 4, it can be noted that the four curves of NDVI–precipitation RR not only overlap each other, but also have relatively stable variation with small fluctuations, reflecting the small differences in NDVI–precipitation similarity of the four stations.

Roughly speaking, the temporal variation patterns of JPR and RR are similar, but JPR can distinguish the finer differences among the four stations. By examining Fig. 5, it is clear that NDVI–temperature synchronization in Station

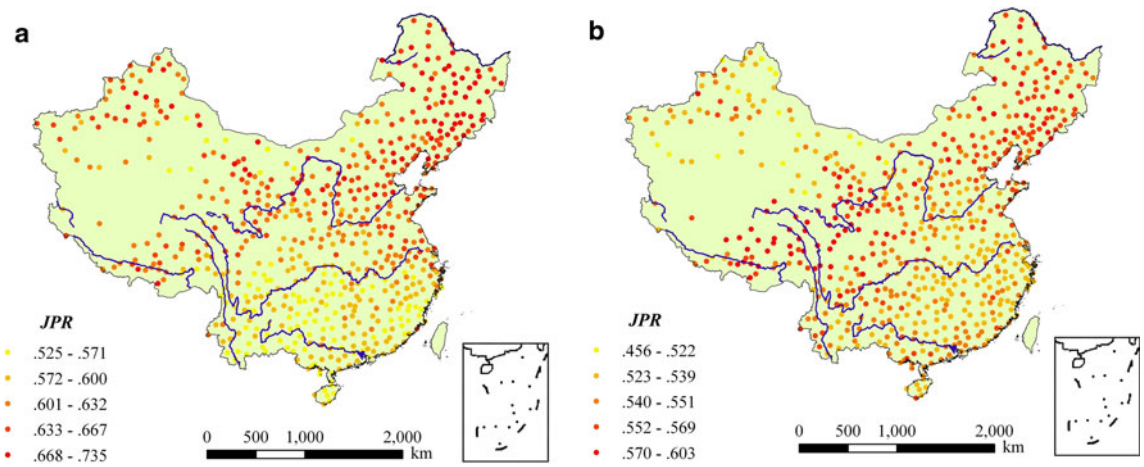

Fig. 2 Spatial pattern of maximal JPR between NDVI and climatic determinants in China. **a** shows the spatial pattern of synchronized relationships between NDVI and temperature, and **b** exhibits regional differentiation of the spatial patterns of synchronized relationships between NDVI and precipitation

Table 1 The geographical characteristics of selected stations

Station code	Longitude	Latitude	Land cover
50968	127°58′E	45°13′N	Temperate deciduous broad-leaved forest
56074	102°05′E	34°00′N	Alpine meadow
58102	115°46′E	33°52′N	Subtropical evergreen broad-leaved forest
59278	112°27′E	23°02′N	Tropical monsoon rain forest

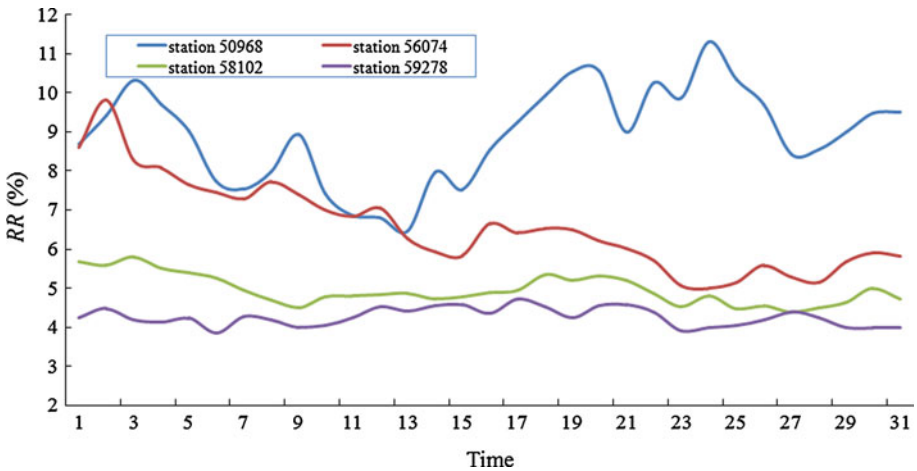

Fig. 3 Temporal variation of RR between NDVI and temperature in selected stations. In figure, 50968, 56074, 58102 and 59278 are four sampling sites in different geographical regions to represent different vegetation types. 50968, temperate deciduous broad-leaved forest; 56074, Alpine meadow; 58102, subtropical evergreen broad-leaved forest; 59278, tropical monsoon rain forest

50968 and Station 56074 is significantly higher than the Station 58102 and Station 59278. In particular, Station 50968 appears the highest synchronization in the middle of the time-varying process. Figure 6 shows clearly how the NDVI–precipitation synchronization varies with time. At most time, Station 50968 and Station 56074 have greater synchronization than the other two stations.

The spatial patterns of lag time of maximal JPR

Generally speaking, NDVI does not respond to immediate temperature and precipitation changes due to the spatial heterogeneity of environmental factors such as topography, vegetation, soil and atmospheric circulation patterns, and temporal variations in temperature and precipitation in different regions of China. To more deeply reveal the regional differentiation of NDVI–climate synchronization, spatial differences in lag time of maximal JPR was computed. As for different meteorological stations, the time lag of NDVI responses to climatic factors is different when the maximal JPR is acquired.

Figure 7a illustrates the spatial distribution of time-lag relationships between NDVI and temperature. The red dotted areas with lag time ranging from −1 to −29 decades

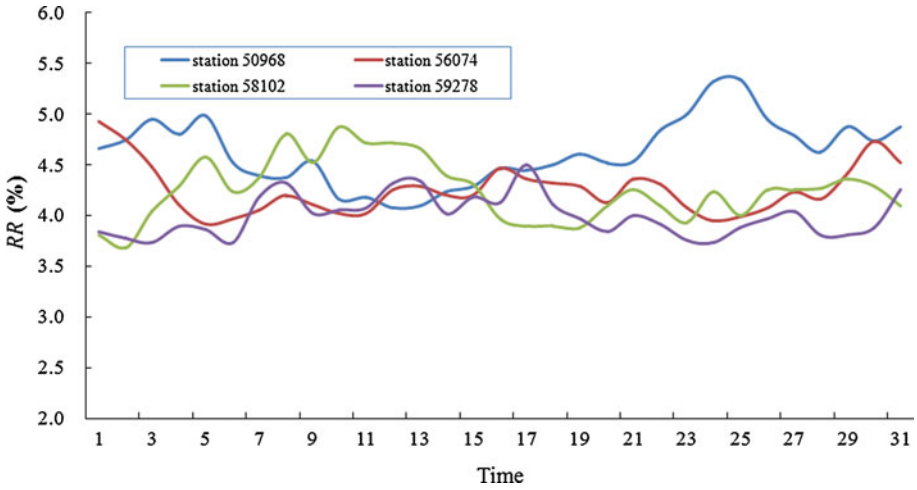

Fig. 4 Temporal variation of RR between NDVI and precipitation in selected stations. In figure, 50968, 56074, 58102, and 59278 are four sampling sites in different geographical regions to represent different vegetation types. 50968, temperate deciduous broad-leaved forest; 56074, Alpine meadow; 58102, subtropical evergreen broad-leaved forest; 59278, tropical monsoon rain forest

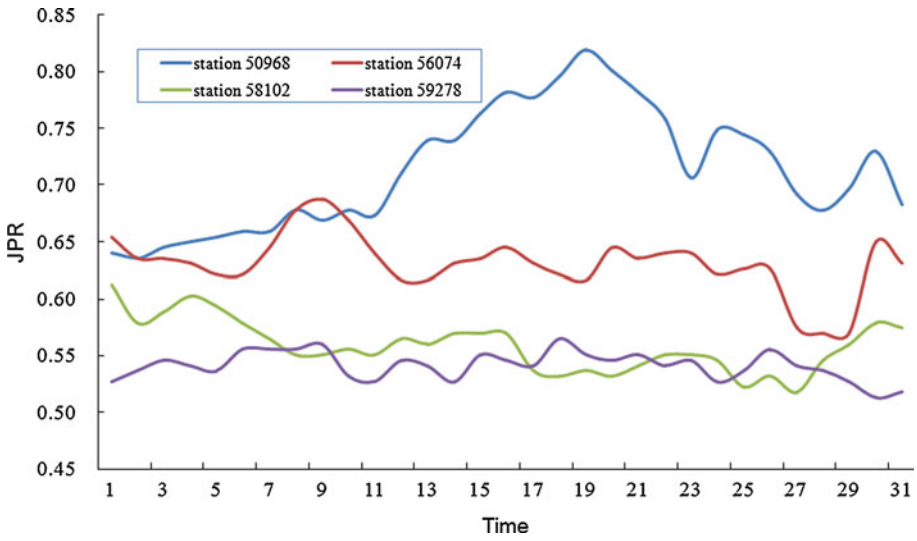

Fig. 5 Temporal variation of JPR between NDVI and temperature in selected stations. In figure, 50968, 56074, 58102, and 59278 are four sampling sites in different geographical regions to represent different vegetation types. 50968, temperate deciduous broad-leaved forest; 56074, Alpine meadow; 58102, subtropical evergreen broad-leaved forest; 59278, tropical monsoon rain forest

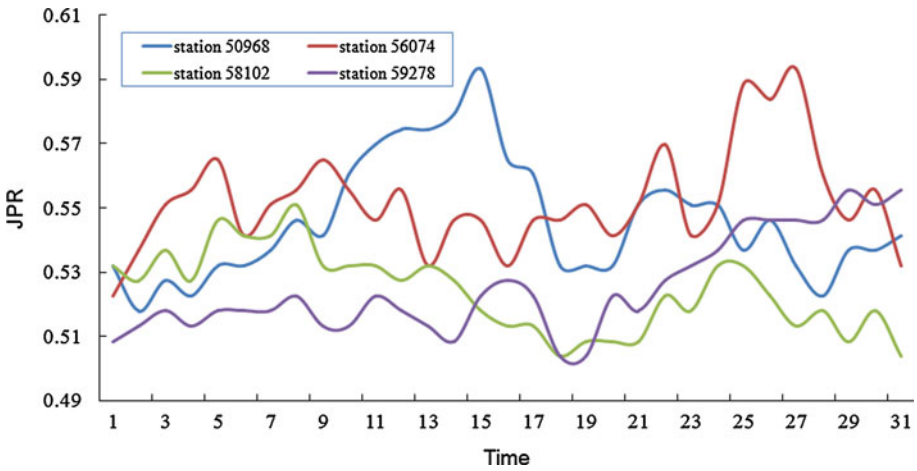

Fig. 6 Temporal variation of JPR between NDVI and precipitation in selected stations. In figure, 50968, 56074, 58102, and 59278 are four sampling sites in different geographical regions to represent different vegetation types. 50968, temperate deciduous broad-leaved forest; 56074, Alpine meadow; 58102, subtropical evergreen broad-leaved forest; 59278, tropical monsoon rain forest

(10 days) dominate the mountainous regions of the Northeast, the central and eastern parts of Inner Mongolia Autonomous Region, the Hebei Plain, the Shandong Peninsula, the central part of the Loess Plateau, central and eastern parts of the Qinghai-Tibetan Plateau, the southern part of Sichuan Province, the southern and northern parts of Yunnan Province, the northern and western parts of Xinjiang Uygur Autonomous Region, Fujian Province,

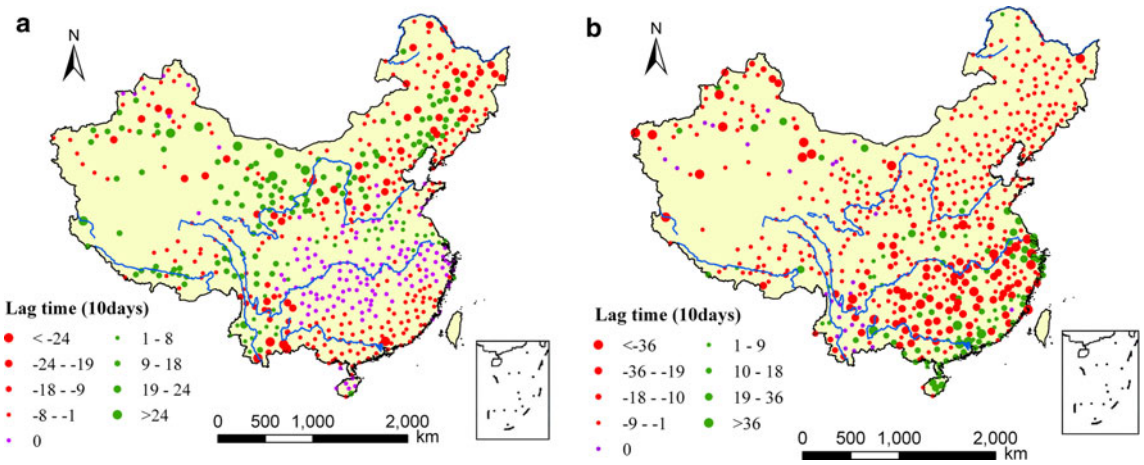

Fig. 7 Spatial patterns of lag time of maximal JPR in China. **a** illustrates the spatial distribution of time-lag relationships between NDVI and temperature, and **b** illustrates the spatial distribution of time-lag relationships between NDVI and precipitation

Guangdong Province, and Guangxi Zhuang Autonomous Region, indicating that the variation of the NDVI series lags behind the temperature series in these areas. Among the above regions, the longest lag time (temperature series leads NDVI series more than 24 ten days) appears in the southern part of Yunnan Province, while the shortest lag time (temperature series leads NDVI series less than 9 ten days) is mainly distributed in the central and eastern parts of Inner Mongolia Autonomous Region, the Shandong Peninsula, central and east parts of the Qinghai-Tibetan Plateau, the southern part of Sichuan Province. The green dotted areas with lag time ranging from 1 to 34 decades (10 days) are mainly distributed at the central and southern parts of the Northeast Plain, the southern part of the Huanghuaihai Plain, the northern and western part of the Loess Plateau, the west part of Sichuan Province, the south and east parts of the Tibetan Autonomous Region, and the central western parts of Yunnan Province, indicating the variation of NDVI series leads the temperature series in these areas. The lead time length of NDVI series prior to temperature series in most of the above regions is 9–24 ten days. The longest lag time values (NDVI series leads temperature series more than 24 ten days) show a scattered distribution in the arid and semi-arid regions of northwestern China, while the shortest lag time values (NDVI series leads temperature series less than 9 ten days) are mainly distributed in the southern part of the Huanghuaihai Plain. The pink dotted areas, representing no lag time between NDVI and temperature, are mainly distributed in Central China, especially in the middle and lower reaches of the Yangtze River, suggesting the variation of NDVI series instantaneously responds to temperature series in these areas.

Figure 7b shows the spatial patterns of lag time of NDVI–precipitation maximal JPR. The red dotted areas show that in most regions of China the NDVI series lags behind the precipitation series. Among these regions, longer time lag (precipitation series leads NDVI series more than 18 ten days) is observed in some regions of Northwestern China and Southern China, while most regions have shorter lag time length (precipitation series leads NDVI series less than 18 ten days), especially in the northeast–southwest zone. The green dotted areas representing NDVI series leads the precipitation series with phase time ranging from 1 to 42 decades (10 days), concentrated in Southern China. The pink dotted areas representing no lag time between NDVI series and precipitation mainly appear in the central parts of Yunnan Province and some regions of Northwestern China, suggesting the synchronous variation of both series in these areas.

Discussion and conclusions

In this study, determination and synchronization of relationships between NDVI–climatic determinants were investigated using JRP and GIS. The conclusions are as follow:

According to the result of RR, the RR values between NDVI and the climatic factors are relatively low, and most of them are under 10%, which indicates that the determination between NDVI and the climatic factors is low. The RR values between NDVI and temperature are higher than that between NDVI and precipitation. The RR values of the four selected stations show the time-varying fluctuations, and the differences of RR between NDVI and temperature among four stations are bigger than those between NDVI and precipitation.

As for the JPR of NDVI–climate, it varies with the different climatic factors. In most areas, the JPR values

between NDVI and temperature are higher than that between NDVI and precipitation, which suggest that the synchronization between NDVI and the temperature is stronger than that between NDVI and the precipitation. The spatial patterns of JPR between NDVI and climatic factors indicate that that JPR is spatially dependent, i.e., different regions have different JPR values. Higher JPR values between NDVI and temperature are located in Northern China, indicating stronger synchronization in these areas, while higher JPR values between NDVI and precipitation are located in semi-arid and semi-humid regions, which means that the moisture factor has the significant influence on NDVI. Similar to the RR, the JPR of the four selected stations show the time-varying fluctuations with significant difference in NDVI–temperature, but only a minor difference in NDVI–precipitation.

Under the condition of maximal JPR, the lagged or advanced relationships between NDVI and climatic factors exhibit significant spatial heterogeneity. Whether lagged or advanced relationship, the phase difference between NDVI and the temperature is smaller in Southern China, while it is bigger in Northern China. In contrast, the phase difference between NDVI and precipitation is smaller in the semi-arid and sub-humid areas, which means that precipitation has significant and immediate influence on vegetation in this area.

Synchronization is an important relationship between vegetation and climatic determinants because it describes coupling strength and phase differences of variation of both systems. The spatial extent and temporal pattern of synchronization can provide information about the extrinsic and intrinsic forces that shape the vegetation-climate relationship. Several studies have illustrated the synchronous relationship between NDVI and climatic determinants. Piao et al. (2003) analyzed the relationship between maxima in NDVI and climatic variables, and confirmed a lagged response of NDVI to changes in climate, which was clearly shown at the country and biome scale. Richard and Poccard (1998) studied the response of NDVI to seasonal and inter-annual rainfall variations in Southern Africa and demonstrated a time response of 1–2 months. By cross-correlation analysis, Prasad et al. (2007) concluded that NDVI–precipitation relationships are site specific and vary according to forest type and period over which they are summed. Although previous studies have found evidence of synchrony between NDVI and climate factors, this is the first study to conclusively demonstrate synchronization of NDVI–climate relationship by using nonlinear measures. The results of the joint recurrence synchronization method are compared with those of the classical cross-correlation method in cases in which the cross-correlation method shows linear spatial cross-dependency, while the joint recurrence synchronization yields nonlinear spatial phase dependency.

The findings on the response of NDVI to climatic determinants are in general agreement with several other studies. For example, Wang et al. (2003) reported the relationship between NDVI to rainfall to be no longer sensitive to rainfall variations beyond a given rainfall threshold, particularly in wet tropical areas. This conclusion can be clearly deduced according to the smaller JPR values and longer response time from Fig. 2b and Fig. 7b in Southern China. In addition, several studies identified surface temperature as a major limiting factor of phonological events in northern latitudes (Zhou et al. 2003; Tateishi and Ebata 2004). This finding can be confirmed according to the larger RR and JPR values from Fig. 1a and Fig. 2a in Northern China.

Whatever the underlying causes may be, the study results of delayed or advanced NDVI response to climatic determinants have significant implications. For example, it can help us better understand the complex relationships between vegetation and climatic factors, which is useful in predicting the dynamics of surface green covers in various climatic scenarios.

Acknowledgments Joint recurrence quantification analysis was done using the cross recurrence toolbox developed by Dr. Norbert Marwan at the Potsdam Institute for Climate Impact Research. The authors gratefully acknowledge his help in providing access to this toolbox. Financial support was provided by National Key Research Development Plan (grant no. 2010CB951704) and National Natural Science Foundation of China, No. 40771001 and No. 40971052.

References

Anyamba A, Tucker CJ (2005) Analysis of Sahelian vegetation dynamics using NOAA-AVHRR NDVI data from 1981–2003. J Arid Environ 63:569–614

Di L, Rundquist DC, Han L (1994) Modelling relationships between NDVI and precipitation during vegetative growth cycles. Int J Remote Sens 15:2121–2136

Eckmann J-P, Kamphorst SO, Ruelle D (1987) Recurrence plots of dynamical systems. Europhys Lett 4:973–977

Fabretti A, Ausloos M (2005) Recurrence plot and recurrence quantification analysis techniques for detecting a critical regime. Examples from financial market indices. Int J Mod Phys C 16:671–706

Fang JY et al (2001) Interannual variability in net primary production and precipitation. Science 293:1723a

Funk CC, Brown ME (2006) Intra-seasonal NDVI change projections in semi-arid Africa. Remote Sens Environ 101:249–256

Goward SN, Tucker CJ, Dye DG (1985) North American vegetation patterns observed with the NOAA-7 advanced very high resolution radiometer. Vegetation 64:3–14

Ichii K, Kawabata A, Yamaguchi Y (2002) Global correlation analysis for NDVI and climatic variables and NDVI trends: 1982–1990. Int J Remote Sens 23:3873–3878

Jarlan L, Mangiarotti S, Mougin E, Mazzega P, Hiernaux P, VLe Dantec (2008) Assimilation of SPOT/VEGETATION NDVI

data into a sahelian vegetation dynamics model. Remote Sens Environ 112:1381–1394
Ji L, Peters AJ (2004) A spatial regression procedure for evaluating the relationship between AVHRR-NDVI and climate in the northern Great Plains. Int J Remote Sens 25(2):297–311
Kaufmann RK et al (2003) The effect of vegetation on surface temperature: A statistical analysis of NDVI and climate data. Geophys Res Lett 30:2147. doi:10.1029/2003GL018251
Li SC, Zhao ZQ, Liu FY (2008) Identifying spatial pattern of NDVI series dynamics using recurrence quantification analysis. Eur Phys J Spec Top 164:127–139
Malo AR, Nicholson SE (1990) A study of rainfall and vegetation dynamics in the African Sahel using normalized difference vegetation index. J Arid Environ 19:1–24
Marwan N, Kurths J (2002) Nonlinear analysis of bivariate data with cross recurrence plots. Phys Lett A 302:299–307
Marwan N, Trauth MH, Vuille M, Kurths J (2003) Comparing modern and pleistocene ENSO influences in NW Argentina using nonlinear time series analysis methods. Clim Dyn 21:317–326
Marwan N, Romano MC, Thiel M, Kurths J (2007) Recurrence plots for the analysis of complex systems. Phys Rep 438:237–329
Maselli F, Chiesi M (2006) Integration of multi-source NDVI data for the estimation of Mediterranean forest productivity. Int J Remote Sens 27:55–72
Myneni RB, Tucker CJ, Asrar G, Keeling CD (1998) Interannual variations in satellite-sensed vegetation index data from 1981 to 1991. J Geophys Res 103:6145–6160
Piao SL, Fang JY, Zhou LM, Guo QH, Henderson M, Ji W (2003) Interannual variations of monthly, seasonal normalized difference vegetation index, (NDVI) in China from 1982 to 1999. J Geophys Res 108(14):4401. doi:10.1029/2002JD002848
Prasad VK, Badarinath KV, Eaturu A (2007) Spatial patterns of vegetation phenology metrics and related climatic controls of eight contrasting forest types in India—analysis from remote sensing datasets. Theor Appl Climatol 89:95–107
Propastin P, Kappas M, Erasmi S (2008) Application of geographically weighted regression to investigate the impact of scale on prediction uncertainty by modeling relationships between vegetation and climate. Int J Spat Data Infra Res 3:73–94
Proulx R, Côté P, Parrott L (2008) Use of recurrence analysis to measure the dynamical stability of a multi-species community model. Eur Phys J Spec Top 164:117–126
Proulx R, Côté P, Parrott L (2009) Multivariate recurrence plots for visualizing and quantifying the dynamics of spatially extended ecosystems. Ecol Complex 6:37–47
Richard Y, Poccard I (1998) A statistical study of NDVI sensitivity to seasonal and interannual rainfall variations in southern Africa. Int J Remote Sens 19:2907–2920
Romano MC, Thiel M, Kurths J, von Bloh W (2004) Multivariate recurrence plots. Phys Lett A 330:214–223
Tateishi R, Ebata M (2004) Analysis of phenological change patterns using 1982–2000 advanced very high resolution radiometer (AVHRR) data. Int J Remote Sens 25:2287–2300
Torres ME, Gamero LG (2000) Relative complexity changes in time series using information measures. Phys A 286:457–473
Tourre YM, Jarlan L, Lacaux J-P, Rotela CH, Lafaye M (2008) Spatio-temporal variability of NDVI–precipitation over southernmost South America: possible linkages between climate signals and epidemics. Environ Res Lett 3. doi:10.1088/1748-9326/3/4/044008
Tucker CJ, Vanpract C, Van Sharman MJ, Ittersum G (1985) Satellite remote sensing of total herbaceous biomass production in the Senegalese Sahel: 1980–1984. Remote Sens Environ 17:233–249
Udelhoven T, Stellmes M, del Barrio G, Hill J (2009) Assessment of rainfall and NDVI anomalies in Spain (1989–1999) using distributed lag models. Int J Remote Sens 30:1961–1976
Wang JM, Rich PM, Price KP (2003) Temporal responses of NDVI to precipitation and temperature in the central Great Plains, USA. Int J Remote Sens 24:2345–2364
Webber CL Jr, Zbilut JP (1994) Dynamical assessment of physiological systems and states using recurrence plot strategies. J Appl Physiol 76:965–973
Xiao JF, Moody A (2004) Trends in vegetation activity and their climatic correlates: China 1982 to 1998. Int J Remote Sens 25:5669–5689
Yang L, Wylie BK, Tieszen LL, Reed BC (1998) An analysis of relationships among climate forcing and time-integrated NDVI of grasslands over the U.S. Northern and Central Great Plains. Remote Sens Environ 98:25–37
Zbilut JP, Giuliani A, Webber CL Jr (1998) Detecting deterministic signals in exceptionally noisy environments using cross-recurrence quantification. Phys Lett A 246:122–128
Zhou L, Kaufmann RK, Tian Y, Myneni RB, Tucker CJ (2003) Relation between interannual variations in satellite measures of northern forest greenness and climate between 1982 and 1999. J Geophpy Res 108:4004